Equilibrium Elasticity of Diblock Copolymer Micellar Lattice

Hiroshi Watanabe,*,† Toshiji Kanaya,† and Yoshiaki Takahashi‡

Institute for Chemical Research, Kyoto University, Uji, Kyoto 611, Japan; and Center for Integrated Research in Science and Engineering, Nagoya University, Nagoya, Aichi 464-8603, Japan

Received May 23, 2000

I. Introduction

Styrene−butadiene (SB) diblock copolymers form spherical micelles with S cores and B corona in a B-selective solvent, *n*-tetradecane (C14). In moderately concentrated solutions where the corona B blocks of neighboring micelles are overlapping each other, these micelles form cubic lattices because of the thermodynamic requirements for the corona B blocks:[1−4] Each corona block is required to randomize its conformation so as to increase the conformational entropy. At the same time, neighboring corona B blocks are osmotically required to have mutually correlated and constrained conformations (with small entropies) so as to minimize the concentration variation in the B/C14 matrix phase and reduce the osmotic free energy. The micellar lattice is formed as a structure that compromises these contradicting requirements. In fact, the lattice is disordered in a polymeric B-selective solvent (homopolybutadiene) that screens the osmotic requirement and allows the corona blocks to randomize their conformations without violating the osmotic requirement.[3,4]

The SB/C14 micellar lattices exhibit equilibrium elasticity against small strains.[1−4] The equilibrium modulus G_e, representing the thermodynamic stability of the lattice,[4] was measured at 25 °C for SB/C14 solutions having various S and B molecular weights (M_S and M_B) and/or various concentrations (c).[1,2] In Figure 1, those G_e data[1,2] are normalized by the thermal energy kT (k = Boltzmann constant and T = absolute temperature) and plotted against the number density ν of the corona B blocks in the solution (unfilled symbols). G_e of those well developed micellar lattices (having various M_S, M_B, and c) are almost proportional to ν, as already pointed out in the previous study.[4] This result suggests that the osmotically constrained corona blocks entropically sustain the equilibrium elasticity.[4]

Since each corona block tethered on the S core has the free end, kinetic effects (such as entanglements) relax/disappear in long time scales where G_e is evaluated. Thus, in the simplest case of the entropic elasticity, each corona block behaves as an independent stress sustaining unit (entropic strand) and its contribution to G_e is given by kT. In Figure 1, the dashed line indicates the equilibrium modulus G_e^o expected for this case

$$G_e^o = \nu kT \tag{1}$$

Clearly, the measured G_e is smaller than this G_e^o by a factor of ∼10. (If we consider the filler effect,[5] the expected G_e^o is larger than that given by eq 1 and the difference from the measured G_e is more prominent.)

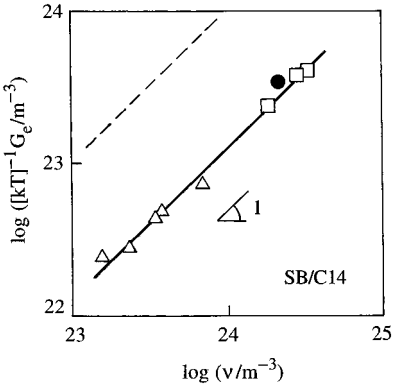

Figure 1. Plots of normalized equilibrium modulus G_e/kT (kT = thermal energy) of SB micellar lattice in *n*-tetradecane (C14) against the number density ν of the corona B blocks. Squares indicate the data previously obtained for SB 16−36/C14 solutions with c = 20, 30, and 35 wt %[1] and the triangles, the data for 10 wt % solutions of SB 20−46, 20−100, 32−102, 32−160, and 32−262,[2] where the sample code numbers indicate $10^{-3}M_S$−$10^{-3}M_B$. The filled circle represents the data of the 15 wt % SB 11−23/C14 solution obtained in this study. All SB micellar lattices were prepared by quiescently cooling the disordered solutions (from $T > T_{ODT}$ to 25 °C) and had the polycrystalline structure. The dashed line indicates the equilibrium modulus expected for the simplest case of entropic elasticity of the corona blocks, $G_e^o = \nu kT$.

The SB micellar lattices examined in Figure 1 were prepared by quiescently cooling the disordered SB/C14 solutions at high temperatures ($T > T_{ODT}$). These lattices unavoidably had polycrystalline structures with many defects, and the above puzzling difference of G_e and G_e^o was vaguely surmised to reflect an effect of the defects.[4] However, no further detail of the difference was discussed in the previous studies.[1−4]

We can examine this difference with the aid of the shear-orientation technique that has been applied to colloidal crystals[6] as well as block copolymers in bulk[7−12] and in micellar solutions.[13−16] The shear-orientated micellar lattice should include less defects compared to the quiescently ordered lattice. *If* the defects are the main factor raising the above difference between G_e and G_e^o, G_e should increase significantly on the shear-orientation.

With the above strategy, we followed McConnell et al.[15] to shear-orient a micellar lattice of a model SB copolymer in C14. Surprisingly, we found that the shear-orientation hardly affects the G_e value and thus the defects are not the main factor raising the difference between G_e and G_e^o. This fact led us to relate this difference to the osmotically induced conformational correlation of neighboring corona B blocks. Details of these results are described in this article.

II. Experimental Section

Material. A styrene-butadiene (SB) diblock copolymer composed of deuterated S and protonated B blocks was synthesized via sequential living anionic polymerization in benzene. The initiator, *sec*-butyllithium, was synthesized from lithium metal and *sec*-butyl bromide (both purchased from Aldrich). The monomers were purified with triphenylmethyl-

* To whom correspondence should be addressed.
† Kyoto University.
‡ Nagoya University.

10.1021/ma000897k CCC: $20.00 © 2001 American Chemical Society
Published on Web 01/05/2001

Table 1. Characteristics of SB Copolymer[a]

code	$10^{-3}M_S$[b]	$10^{-3}M_B$[c]	M_w/M_n[d]
SB 11-23	11.1	23.0	1.04

[a] Composed of deuterated S and protonated B blocks. [b] Determined from GPC elution calibration for the precursor S block after correction of the difference of the monomer molecular weights for deuterated and protonated S. (M_w/M_n = 1.03 for the S block.) [c] Evaluated from M_S of the S block and the B weight fraction in the copolymer, with the latter being determined from RI and UV signals. [d] Evaluated from GPC elution calibration for the copolymer.

lithium (for S from Aldrich) and *sec*-butyllithium (for B from Tokyo Kasei).

The SB copolymer and its precursor S block (recovered before the copolymerization of the B block) were characterized with GPC (CO-8020 and DP-8020, Tosoh) equipped with refractive index (RI) and ultraviolet adsorption (UV) monitors (LS-8000 and UV-8020, Tosoh) connected in series. Monodisperse polystyrenes (Tosoh TSK's) were utilized as elution standards.

Table 1 summarizes the characteristics of the SB sample (coded as SB 11−23). The system examined was a SB 11−23 solution in *n*-tetradecane (C14). This solution was prepared from a homogeneous solution of SB 11−23 and C14 in excess benzene by allowing benzene to thoroughly evaporate. The SB concentration in the SB/C14 solution, determined after this evaporation, was 15 wt %. In this solution at 25 °C, spherical micelles with glassy S cores and solvated B corona formed the bcc lattice, as noted from the small-angle neutron scattering (SANS) profile shown later.

Measurements. For the 15 wt % SB 11−23/C14 solution at 25 °C, rheological measurements were carried out with a laboratory rheometer (RMS605, Rheometrics). A Couette flow cell with radii of the inner and outer cylinders, r_i = 25.0 mm and r_o = 26.0 mm, respectively, was utilized (so that the flow geometry was similar to that in shear-SANS measurements).

In SANS measurements, we utilized the SANS−U beam line at the Neutron Scattering Laboratory, Institute for Solid State Physics, University of Tokyo (Tokai, Ibaragi, Japan) in the following configuration: incident neutron wavelength λ = 0.7 nm, wavelength spread $\Delta\lambda/\lambda$ = 0.1, sample-to-detector distance = 4.00 m, and beam diameter = 0.3 cm. The scattering intensity was measured as a function of the scattering vector $\mathbf{q}$, where $q = |\mathbf{q}| = [4\pi/\lambda] \sin(\theta/2)$, with θ being the scattering angle.

The SANS measurements were carried out at room temperature (≅25 °C) for the SB 11−23/C14 solution in a Couette flow cell[17] with r_i = 25.25 mm and r_o = 27.00 mm. For the quiescently ordered solution (prepared by cooling the solution from $T > T_{ODT}$ to 25 °C), the SANS profiles were obtained before, during, and after imposition of the steady shear flow. The incident beam was in the direction normal to the surfaces of the inner/outer cylinders of the cell (i.e, in the direction of the velocity gradient), and the profiles were detected in a velocity−vorticity (x−y) plane. (Thus, the total sample thickness for the scattering was 3.5 mm.) With the above configuration, the scattering was detected in a range of q_x and q_y, $|q_x| \le 0.71$ nm^{-1} and $|q_y| \le 0.71$ nm^{-1}. No correction was made for the incoherent scattering.

III. Results and Discussion

III-1. Shear Orientation. For the face- and body-centered cubic (fcc and bcc) lattices of styrene−isoprene (SI) diblock copolymer micelles in *n*-decane (C10; I-selective solvent), McConnell et al.[15] examined SANS profiles during flow at various shear rates $\dot\gamma$. They found that the long-range order of both lattices change with $\dot\gamma$ and these changes (of the fcc lattice) are correlated with the quasi-stationary shear stress σ.[15] We attempted to utilize their results as a clue to find the optimum $\dot\gamma$ value for achieving the long-range order in our SB micellar lattice.

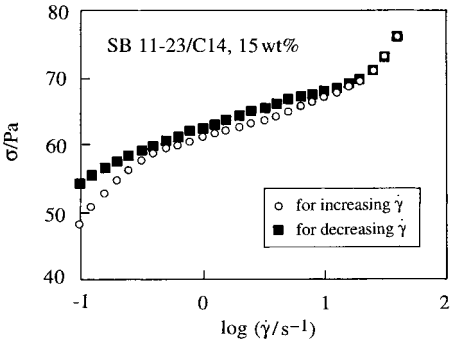

Figure 2. Flow behavior of the 15 wt % SB 11−23/C14 solution at 25 °C. The unfilled and filled symbols indicate the quasi-stationary shear stress measured for increasing and decreasing $\dot\gamma$, respectively.

For this purpose, we followed McConnell et al.[15] to examine the flow behavior of our SB 11−23/C14 solution. The results are shown in Figure 2. The unfilled and filled symbols indicate the quasi-stationary σ data obtained for increasing and decreasing $\dot\gamma$, respectively. The hysteresis, seen for these two sets of σ data at $\dot\gamma <$ 20 s^{-1}, disappears at higher $\dot\gamma$. With decreasing $\dot\gamma$, σ decreases significantly in the nonhysteresis regime and less prominently in the hysteresis regime. These features are similar to those found for the fcc-type SI micellar solution,[15] (although this SI solution also exhibited small but abrupt drops of σ that are not observed for our bcc-type SB micellar solution).

The fcc lattice of the SI micelles examined by McConnel et al.[15] appears to be best oriented at $\dot\gamma$ a little smaller than the threshold $\dot\gamma$ value between the hysteresis and nonhysteresis regimes. The threshold for our bcc-type SB micellar lattice is at $\dot\gamma \sim$ 20 s^{-1} (Figure 2). Thus, we chose $\dot\gamma$ = 10 s^{-1} and examined the shear-orientation of our SB lattice at this $\dot\gamma$. The results are shown in Figure 3. The panels show the SANS profiles each obtained with the exposure time of 10 min. The horizontal and vertical (x and y) directions correspond to the velocity and vorticity directions of the shear flow.

The quiescently ordered SB micellar lattice was prepared in the SANS flow cell by cooling the 15 wt % SB 11−23/C14 solution from high T ($> T_{ODT}$) to 25 °C. Essentially *isotropic* scattering peaks are observed at q = 0.22, 0.32, and 0.38 nm^{-1}; cf. the left panel of Figure 3. (The stronger scattering in the x direction results from a weak lattice orientation due to the sample shrinkage in the cell on cooling.) The ratio of these q values is very close to $1:\sqrt{2}:\sqrt{3}$. These results indicate that the quiescently ordered solution has the isotropically orientated bcc polycrystalline structure (with the lattice spacing $D \cong$ 35 nm). This polycrystalline structure should include many *defects*.

Under the steady shear at $\dot\gamma$ = 10 s^{-1}, the scattering pattern drastically changes to the anisotropic pattern (middle panel of Figure 3). A similar pattern was found for the bcc-type SI micellar lattice under flow and assigned as the scattering from the locally distorted ⟨110⟩ plane.[15] The long-range order of the SB lattice (reflected in the pattern anisotropy) is enhanced when the solution is kept quiescently after cessation of the steady shear, as seen in the right panel of Figure 3 (obtained 50 min after the cessation). Thus, the orien-

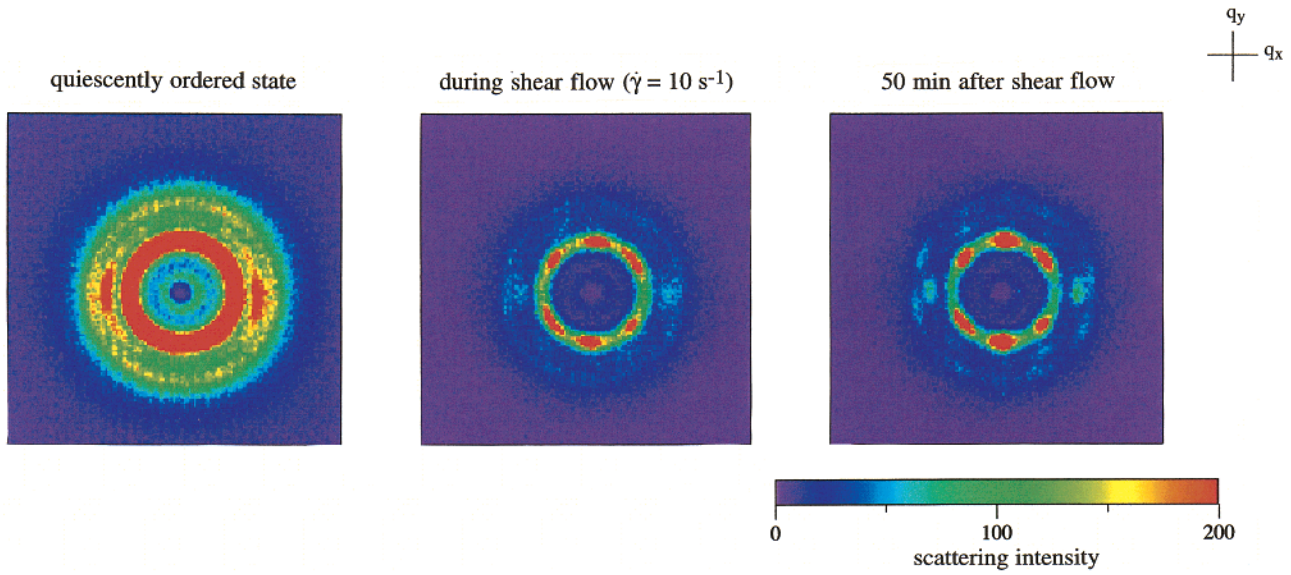

Figure 3. SANS profiles of the 15 wt % SB 11−23/C14 solution at 25 °C. The quiescently ordered SB micellar lattice has the polycrystalline bcc structure (left panel). This lattice is oriented under steady shear flow at $\dot{\gamma} = 10$ s^{-1} (middle panel), and the long-range order of this lattice is enhanced when the solution is quiescently kept for 50 min after cessation of the shear (right panel). Each profile, covering $|q_x| \leq 0.71$ nm^{-1} and $|q_y| \leq 0.71$ nm^{-1}, was obtained with an exposure time of 10 min.

tated SB lattice with less defects was successfully obtained after the shear at $\dot{\gamma} = 10$ s^{-1}.

We also examined different $\dot{\gamma}$ values but obtained less orientated SB micellar lattice. In particular, the shear-melting occurred under the flow at high $\dot{\gamma}$ (=100 s^{-1}), as similar to the result reported for the bcc-type SI micelles.[15] Thus, the shear at $\dot{\gamma} = 10$ s^{-1} gave the best orientated SB micellar lattice that quite possibly included the smallest amount of defects.

III-2. Equilibrium Modulus of SB Micellar Lattices. On the basis of the above SANS results, we compared the linear viscoelastic responses of the quiescently ordered bcc polycrystalline lattice with those of the best orientated bcc lattice obtained after the steady shear at $\dot{\gamma} = 10$ s^{-1}. These two lattices were prepared in the Couette cell of the rheometer under the conditions/treatments very similar to those in the flow-SANS experiments. Specifically, the viscoelastic measurement for the oriented lattice was started 50 min after cessation of the steady shear and completed in 10 min (the exposure time for the SANS profile). Thus, the rheologically examined lattices should have been very similar to those detected in the SANS profiles (left and right panels of Figure 3).

Figure 4 shows plots of the storage moduli G' of the above two lattices against the angular frequency ω of the oscillatory strain. Filled squares and unfilled circles indicate G' of the quiescently ordered (polycrystalline) and shear-oriented lattices, respectively. G' is insensitive to ω (<10 s^{-1}), demonstrating the elastic responses of both lattices. (Correspondingly, the loss moduli G'' were much smaller than G' at those ω). Thus, the equilibrium modulus G_e of the lattice was evaluated as the G' at the lowest ω examined. For the polycrystalline SB micellar lattice, this G_e is plotted against the number density of the corona B blocks in Figure 1 (filled circle). We note good agreement with the previous data (unfilled symbols).

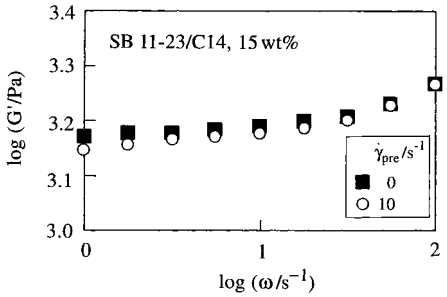

Figure 4. Storage moduli G' of the polycrystalline bcc micellar lattice (filled square) and shear-oriented lattice (unfilled circles) in the 15 wt % SB 11−23/C14 solution at 25 °C. These lattice structures correspond to those seen in left and right panels of Figure 3.

As seen in Figure 4, the difference of the G_e values of the polycrystalline and well oriented lattices is surprisingly small (less than 10%).[18] Furthermore, for the lattices differently shear-oriented at various $\dot{\gamma}$ (not shown here), the G_e value differed only by a factor <20%. These results indicate that the G_e of the oriented lattice, quite possibly including less defects compared to the polycrystalline lattice, is still smaller, by a factor of ~10, than the G_e^o expected for the simplest case of entropic elasticity of the B corona (eq 1).

The G_e of the oriented lattice represents the elasticity along a particular lattice plane and does not necessarily correspond to the largest modulus exhibited by the lattice. If a continuous, flowing plane formed under the steady shear survives after cessation of the shear, G_e may become smaller than G_e^o. However, as judged from the shear effect seen in Figure 4, these factors do not seem to be sufficient for decreasing the G_e of the oriented lattice from G_e^o down to ~G_e^o/10. Thus, we may conclude that the defects could have a secondary effect on G_e but are not the main factor raising the large difference between G_e and G_e^o.

Here, we remember that the B blocks in the SB/C14 solution are required to have mutually correlated, constrained conformations to minimize the osmotic energy, and the micellar lattice is formed due to this osmotic requirement. Thus, by nature, all corona B blocks sustaining the micellar lattice cannot work as the *independent* entropic strands.

This argument suggests that the number density ν_{eff} of effectively working entropic strands is smaller than the nominal number density ν of the corona B blocks and G_e of the micellar lattice is given by $\nu_{eff}kT$ ($< G_e^o = \nu kT$; cf. eq 1). The difference between G_e and G_e^o appears to be mainly due to the difference between ν_{eff} and ν (although no quantitative explanation has been obtained for the ν_{eff}/ν ratio suggested from Figure 1, $\nu_{eff}/\nu \cong 0.1$).

In relation to the above conformational correlation, we expect an interesting solvent effect on the elasticity. In ordered ABC-type triblock copolymer systems, the middle B block bridges the A and C domains. For these middle B blocks swollen with a B-selective solvent, the elasticity is expected to be enhanced when the solvent screens the osmotic interaction of those blocks thereby allowing them to work as independent entropic strands.[19] This expectation is in harmony with recent experiments for a styrene−isoprene−2-vinylpyridine (SIP) triblock copolymer in monomeric and polymeric I-selective solvents, *n*-tetradecane and low-*M* homopolyisoprene, the latter screening the osmotic interaction of the I blocks.[20]

We also expect that the G_e/G_e^o ratio ($=\nu_{eff}/\nu$ ratio) of the micellar lattice is determined by the degree of the conformational correlation of neighboring corona blocks and may change with the solvent quality (solubility toward the corona block). It would be interesting to examine a correlation between the G_e/G_e^o ratio and the solvent quality. This is considered as an interesting subject for future work.

IV. Concluding Remarks

Attempting to elucidate the origin of the large difference between the measured equilibrium modulus of SB micellar lattices G_e and the modulus G_e^o ($=\nu kT$) expected for the simplest case of the entropic elasticity of the corona B blocks, we compared the G_e values of a quiescently ordered, polycrystalline lattice and a shear-orientated lattice (including less defects). The difference of the G_e's of these lattices was surprisingly small (less than 10%) and the G_e of the oriented lattice was still smaller than G_e^o by a factor of ∼10. This result suggests that the defects are not the main factor raising the difference between G_e and G_e^o. This fact led us to attribute the difference to the osmotic constraint for the corona conformation: This constraint, the driving force of the micellar lattice formation, results in conformational correlation of the corona blocks. This correlation quite possibly reduces the effective number density ν_{eff} of independently working entropic strands ($\nu_{eff} < \nu$) thereby giving G_e ($=\nu_{eff}kT$) smaller than G_e^o.

References and Notes

(1) Watanabe, H.; Kotaka, T.; Hashimoto, T.; Shibayama, M.; Kawai, H. *J. Rheol.* **1982**, *26*, 153.
(2) Watanabe, H.; Kotaka, T. *Polym. J.* **1982**, *14*, 739.
(3) Watanabe, H.; Kotaka, T. *J. Rheol.* **1983**, *27*, 223.
(4) Watanabe, H. *Acta Polym.* **1997**, *48*, 215.
(5) Guth, E. *J. Appl. Phys.* **1945**, *16*, 20.
(6) Chen, L. B.; Chow, M. K.; Ackerson, B. J.; Zukoski, C. F. *Langmuir* **1994**, *10*, 2817.
(7) Bates, F. S.; Rosedale, J. H.; Fredrickson, G. H. *J. Chem. Phys.* **1990**, *92*, 6255.
(8) Koppi, K. A.; Tirrell, M.; Bates, F. S.; Almdal, K.; Colby, R. H. *J. Phys. II (Fr.)* **1992**, *2*, 941.
(9) Larson, R. G.; Winey, K. I.; Patel, S. S.; Watanabe, H.; Bruinsma, R. *Rheol. Acta* **1993**, *32*, 245.
(10) Patel, S. S.; Larson, R. G.; Winey, K. I.; Watanabe, H. *Macromolecules* **1995**, *28*, 4313.
(11) Koppi, K. A.; Tirrell, M.; Bates, F. S.; Almdal, K.; Mortensen, K. *J. Rheol.* **1994**, *38*, 999.
(12) Zhao, J.; Majumdar, B.; Schulz, M. F.; Bates, F. S.; Almdal, K.; Mortensen, K.; Hajduk, D. A.; Gruner, S. M. *Macromolecules* **1996**, *29*, 1204.
(13) Mortensen, K.; Brown, W.; Nordén, B. *Phys. Rev. Lett.* **1992**, *68*, 2340.
(14) Phoon, C. L.; Higgins, J. S.; Allegra, G.; Van Leeuwen, P.; Staples, E. *Proc. R. Soc. London A* **1993**, *442*, 221.
(15) McConnell, G. A.; Lin, M. Y.; Gast, A. P. *Macromolecules* **1995**, *28*, 6754.
(16) For block copolymers, the shear orientation behavior is summarized in a recent review: Watanabe, H. Rheology of Multiphase Polymeric Systems. In *Structures and Properties of Multiphase Polymeric Materials*; Araki, T., Tran-Cong, Q., Shibayama, M., Ed.; Marcel Dekker: New York, 1998; Chapter 9, pp 317−360.
(17) Takahashi, Y.; Noda, M.; Naruse, M.; Kanaya, T.; Watanabe, H.; Kato, T.; Imai, M.; Matsushita, Y. *J. Soc. Rheol. Jpn.* **2000**, *28*, 187.
(18) The very small effect of shear-orientation on G_e of the micellar lattice (Figure 4) is in contrast to the huge effect observed for the block copolymers having lamellar and/or cylindrical domains:[7−11] The G' (or G_e) measured along the lamellar plane and/or cylindrical axis is much smaller than the G' of polygrain lamellae/cylinders. This difference between the micellar lattice and lamellae/cylinder is related to the difference in their translational symmetries:[16] The cubic arrangement of the micelles is distorted by a static strain in any direction, while the lamellar and/or cylindrical arrangement is not affected by the strain in the directions along the lamellar surface and/or cylindrical axis. The equilibrium elasticity emerges when the static strain distorts the domain arrangements.
(19) The corona block of the diblock copolymer micelle has the tail conformation with the free end. Thus, these blocks fully relax and sustain no equilibrium elasticity in solvents that screen the osmotic interaction: In such solvents, the micellar lattice is disordered and the system flows viscoelastically, as confirmed for the SB micellar solution in low-*M* polybutadiene (a polymeric B-selective solvent).[3,4] On the other hand, the middle block of the ABC triblock copolymer has the bridge conformation and sustains the equilibrium elasticity even in those solvents. Thus the equilibrium elasticity of those middle blocks is enhanced when the osmotic interaction is screened, as observed for a SIP copolymer in low-*M* polyisoprene (a polymeric I-selective solvent).[20.]
(20) Watanabe, H.; Sato, T.; Osaki, K. Manuscript in preparation.

MA000897K